第 49 卷 第 10 期
2022 年 10 月

湖南大学学报（自然科学版）
Journal of Hunan University (Natural Sciences)

Vol. 49 No. 10
October 2022

Open Access Article https://doi.org/10.55463/issn.1674-2974.49.10.5

Experimental Approach to Developing Equatorial Soil Loss Equation

Samuel Lik Ging Law[1], King Kuok Kuok[1]*, Shirley Gato Trinidad[2], Po Chan Chiu[3], Md. Rezaur Rahman[4], Muhammad Khusairy Bin Bakri[5], Mei Yun Chin[1]

[1] Faculty of Engineering, Computing and Science, Swinburne University of Technology Sarawak Campus, Kuching, Malaysia

[2] Centre for Sustainable Infrastructure and Digital Construction, Department of Civil and Construction Engineering, Swinburne University of Technology, Hawthorn, Australia

[3] Faculty of Computer Science and Information Technology, Universiti Malaysia Sarawak, Kota Samarahan, Sarawak, Malaysia

[4] Faculty of Engineering, Universiti Malaysia Sarawak, Kota Samarahan, Sarawak, Malaysia

[5] Composites Materials and Engineering Center, Washington State University, 2001 East Grimes Way, Pullman, Washington State, USA

Abstract: This paper aims to develop a soil loss equation used within an equatorial climate (2,300 – 6,000 mm of annual rainfall) and hilly terrain based on measured data from the experiment concerning measured erosion outcomes, called Equatorial Soil Loss Equation (EQSLE). The equation under development should consider high equatorial rainfall intensities and challenging topographical conditions, thus introducing the new factors – Equatorial Rainfall Erosivity Factor (R_{eqt}-factor) and Equatorial Slope Length Factor (L_{eqt}-factor). The process included a photogrammetric method and image processing for raindrop size distribution and an experimental plot setup for a length differential study. The final equation has the form of $A=R_{eqt}\square L_{eqt}\square S\square K\square C\square P$ for soil erosion estimation in the equatorial region with the involvement slope and hilly terrain. The performance of the R_{eqt}-factor and L_{eqt}-factor are evaluated using the experimental data, and works of literature are carried out for the results. The formation of the two factors has addressed the challenges of high rainfall intensities and extreme terrain conditions faced by Peninsular Malaysia and East Malaysia. In future work, more case studies on the performance of soil loss rate prediction should be conducted to improve the overall performance of EQSLE as well as the respective factors.

Keywords: equatorial rainfall erosivity factor, equatorial slope length factor, photogrammetric method, image processing tools.

建立赤道土壤流失方程的實驗方法

摘要：本文旨在根據有關測量的侵蝕結果的實驗測量數據，開髮用於赤道氣候（年降雨量 2,300–6,000 毫米）和丘陵地形的土壤流失方程，稱為赤道土壤流失方程。開發中的方程應考慮赤道高降雨強度和具有挑戰性的地形條件，從而引入新的因子——赤道降雨侵蝕係數（R_{eqt}-因素）和赤道坡長因子（L_{eqt}-因素）。該過程包括用於雨滴尺寸分佈的攝影測量方法和圖像處理，以及用於長度差異研究的實驗樣地設置。最終方程的形式為 $A=R_{eqt}\square L_{eqt}\square S\square K\square C\square P$，用於赤道地區涉及坡地和丘陵地形的土壤侵蝕估算。$R_{eqt}$-因素和 L_{eqt}-因素的性能使用實驗數據進行評估，並對結果進行文獻研究。這兩個因素的形成解決

Received: July 16, 2022 / Revised: August 13, 2022 / Accepted: September 18, 2022 / Published: October 30, 2022

Fund Project: The Ministry of Education Malaysia (Fundamental Research Grant Scheme (FRGS) (Reference Code: FRGS/1/2019/TK01/SWIN/02/1))

About the authors: Samuel Lik Ging Law (PhD Candidate), King Kuok Kuok (Associate Professor), Faculty of Engineering, Computing and Science, Swinburne University of Technology Sarawak Campus, Kuching, Malaysia; Shirley Gato Trinidad (Associate Professor), Centre for Sustainable Infrastructure and Digital Construction, Department of Civil and Construction Engineering, Swinburne University of Technology, Hawthorn, Australia; Po Chan Chiu (Lecturer), Faculty of Computer Science and Information Technology, Universiti Malaysia Sarawak, Kota Samarahan, Malaysia; Md. Rezaur Rahman (Senior Lecturer), Faculty of Engineering, Universiti Malaysia Sarawak, Kota Samarahan, Malaysia; Muhammad Khusairy Bin Bakri (Postdoctoral Research Associate), Composites Materials and Engineering Center, Washington State University, Pullman, Washington, USA; Mei Yun Chin (Lecturer), Faculty of Engineering, Computing and Science, Swinburne University of Technology Sarawak Campus, Kuching, Malaysia

Corresponding author King Kuok Kuok, kkuok@swinburne.edu.my

了馬來西亞半島和東馬面臨的高降雨強度和極端地形條件的挑戰。在未來的工作中，應該對土壤流失率預測的性能進行更多的案例研究，以提高赤道土壤流失方程的整體性能以及各個因素。

关键词：赤道降雨侵蝕力因子、赤道坡長因子、攝影測量方法、圖像處理工具。

1. Introduction

1.1. Background

Soil erosion models are useful for predicting soil loss and runoff rates from sites such as agricultural land or development areas. According to Smith [1], it provides relative soil loss information, especially in the Erosion and Sediment Control Plan (ESCP), and guides government policy and soil and water conservation strategy. Various soil erosion models are currently applicable around the globe, including the Water Erosion Predict Project (WEPP) [2], Griffith University Erosion System Template (GUEST) [3], the European Soil Erosion Model (EUROSEM) [4], Limburg Soil erosion Model (LISEM) [5]. Although many soil erosion models had been developed with related experiments in the early 1900s, the models were limited to explore a broader region. The data collected for the models were based on local conditions and the data are only applicable to local conditions with respect to the soil erosion models.

The limitations of soil loss models were further improved by introducing the ideas of soil loss factors that act as the vital fundamentals of soil loss processes. The soil loss factors have been compounded and form the soil loss equation. The parameters that influence erosion that considers are rainfall, slope length, slope steepness, vegetation cover, soil properties and erosion control methods [1]. Various researchers have examined the revolution and improvement of the soil loss equation since the late 1900s. Different versions of the soil loss equations have been developed and published, including Universal Soil Loss Equation (USLE) [6] and Revised Universal Soil Loss Equation (RUSLE) [7].

The soil loss equations are developed empirically using massive field data and concluded in an equation. According to [8], the developed equation is expected to provide a reliable estimation of soil erosion; some researchers (the authors of studies [9-12]) have attempted to evaluate the equation, but very few conclusions could be drawn on the overall accuracy of the equation. The authors of [13-15] also suggested that the soil erosion equation tends to underestimate soil erosion on rangeland plots. Their findings assume that the performance of soil loss equations is often influenced by climate and topographical conditions. The soil loss equations developed locally would have more impact on soil erosion prediction than the direct application of soil loss equations from the other region.

1.2. Problem Statement

Two of the main parameters that highly influence the soil erosion outcomes are the rainfall erosivity index and the topographical condition of the site. The nature formation of the topographical conditions in Malaysia, especially in East Malaysia (Sarawak and Sabah) is unique with many high terrains with critical slopes. The hilly topography of Sarawak has been supported by [16] and [17]. A few locations around Peninsular Malaysia and East Malaysia had been previously studied on their soil erosion condition and assessment on soil erosion risk as shown in Table 1 and the severity of soil erosion has been classified into Low, Moderate, High and Critical according to [18].

Table 1 Soil erosion assessment at highlands locations in Malaysia

Source	Location	Soil Erosion Rate, ton ha^{-1} yr^{-1}	Soil Erosion Risk
[19]	Tasik Chini Catchment, Pahang	111.4	High
[20]	Tikolod, Sabah	303.1	Critical
[18]	Mukim Hulu Telom, Cameron Highlands	327.0	Critical
[21]	Batu Kayu, Hitam, Johor Bahru	678.0	Critical
	Mukim Bringchang, Cameron Highlands	488.0	Critical
	Mukim Ringlet, Cameron Highlands	365.0	Critical

Climate conditions in Malaysia experience high rainfall intensity throughout the year, and studies have shown that approximately 2,300 – 6,000 mm of annual rainfall can be collected in Peninsular Malaysia and East Malaysia [22, 23]. It could be higher during the monsoon; especially during the North-East Monsoon (November to March) and South-West Monsoon (May to September) [24]. Malaysia is located between the latitudes of 1°N and 7°N that fall within the definition of "Sub-tropical" or "Equatorial Region" and experiences mainly equatorial climate with high rainfall intensity [25, 26]. Table 2 shows the comparison of mean annual rainfall and rainfall intensities in different regions of the world and Fig. 1.3

shows the Köppen-Geiger climate classification world map [27].

Table 2 Mean annual rainfall and rainfall intensity at different regions

Region	Latitude	Mean Annual Rainfall (mm)	Rainfall Intensity (mm/hr)	Sources
Polar	66.5° - 90°N	< 600	0.1 – 11	[34]
	66.5° - 90°S			[35]
Temperate	35° - 66.5°N	200 – 2000	1 – 75	[36]
	35° - 66.5°S			[37]
Sub-tropical	23.5° - 35°N	100 – 2500	1 – 150	[38]
	23.5° - 35°S			[39]
Tropical	5° - 23.5°N	1000 – 4000	25 – 175	[38]
	5° - 23.5°S			[39], [40]
Equatorial	0° - 5°N	2000 – 6000	49 – 200	[38]
	0° - 5°S			[41]

These two crucial erosion parameters have highlighted a need to develop a suitable soil loss equation that would assure the accuracy of the prediction of erosion rate under equatorial climate and critical terrain faced in Peninsular Malaysia and East Malaysia. This study develops a soil loss equation used within an equatorial country like Malaysia, based on measured data from experimental soil plots and equatorial climate data with respect to measured erosion outcomes, which is called Equatorial Soil Loss Equation (EQSLE).

2. Methodology

The methodology of this study involves several different experimental procedures to determine the new formation of Equatorial Rainfall Erosivity Factor (R_{eqt}-factor) and Equatorial Slope Length Factor (L_{eqt}-factor). The experiments focus on the properties of equatorial rainfall, especially on the high rainfall intensity properties and its impact on the ground that initiates soil erosion processes. Different slope lengths are designed to study the changes in soil erosion outcomes based on different slope length, thus proceeding to the formation of the L_{eqt}-factor. The selected site was located in Malaysia, Kuching, in Sarawak, a city with a tropical rainforest climate [28, 29]. It is approximately 2.46 km from Swinburne University of Technology Sarawak Campus with a coordinate of 1°32’ 47.99” N, 110° 22’ 26.37” E (Fig. 1). A standard tipping bucket rain was installed onsite to collect rainfall data, duration, and daily rainfall. The data were monitored in the real-time experiment.

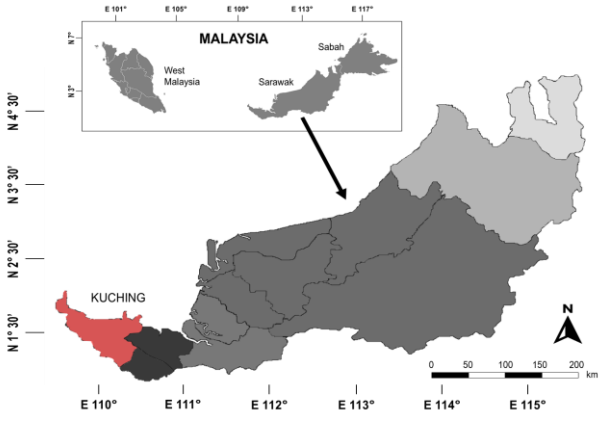

Fig. 1 Locality map

2.1. Setup of Experimental Soil Plots

Experimental soil plots (Fig. 2) with different plot lengths were constructed with three dimensions 1 × 1 m plot, 1 × 2 m plot, and 1 × 3 m plot. The structures and dimensions were designed to adequate height to collect runoffs. An angle of 22.78° from the horizontal was designed for all three plots. The purpose of the design is to ensure that the runoff during low rainfall intensity storm events. Other than consistent runoffs, a constant value for the slope angle would help fix the value for Slope Steepness Factor (S-factor). The soil sample used for the experiment falls under the definition of homogenous topsoil with no addition of sand or organic materials. The soil sample was tested for its particle size distribution and soil properties. The tested information could be applied to calculate Soil Erodibility Factor (K-factor). A constant soil type would help fix a constant K-factor value throughout the experiment. The soil's surface loaded in the test bay would keep it bare to simulate similar conditions for the Cover Management Factor (C-factor). No additional soil erosion protection procedures are taken on the experimental plot to keep constant for the Support Practices Factor (P-factor).

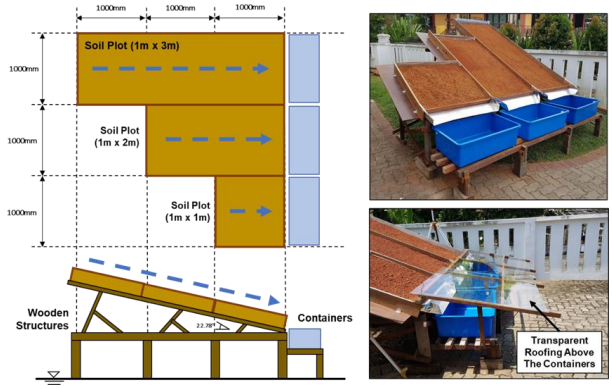

Fig. 2 Experimental plot setup

2.2. Setup of Raindrop Photogrammetry

The setup of raindrop photogrammetry is shown in Fig. 3. A professional DSLR camera (Sony α6000) captured the natural rainfall droplet distribution. Suitable adjustments on camera settings (ISO, aperture, shutter speed, focal length) were performed during the photo shooting process to produce sharp images of

raindrop sizes. A larger number of raindrop photographs were taken for the individual rainfall events to capture representative raindrop distribution patterns. A customized rainfall photobooth with a dark background was fabricated to capture the individual droplet sizes during a rainfall event. A customized coding script program processed the selected images, including the droplet image, and was run in MATLAB for image segmentation. The processed images provided the information on raindrop count; drop diameter, drop area, drop perimeter and coordinates of the raindrops and the numeral data were extracted and subsequently categorized into several intervals for raindrop size distribution analysis. The raindrop size distribution of a specific rainfall event would be scaled to the size of a storm event to analyze the overall distribution of kinetic energy in the rainfall event. The determination of the raindrop energy would be based on a similar fundamental as the kinetic energy equation. The R_{eqt}-factor equation is developed from the fundamentals of the kinetic energy equation.

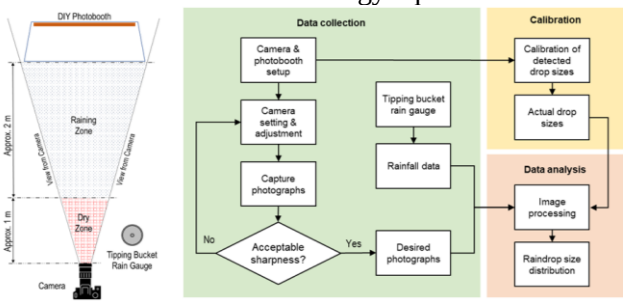

Fig. 3 Raindrop photogrammetry setup and flowchart for raindrop data collection process

After the images were removed from the experimental site, photos with clearer resolution and clarity were selected and processed using image processing tools in MATLAB. The image processing procedures consisted of a few stages of image conversion, as shown in Fig. 4. It was adjusted and cropped to the ideal size from the original image to process the image in a smaller file size, thus increasing the processing speed in MATLAB. The cropped image was processed into a grayscale image, colored image, labeled image, and binary image. The complete analysis is carried out in MATLAB and the outputs are extracted including the number of blobs, k, mean intensity (pixel), areas of blobs (pixel), the perimeter of the blobs (pixel), the centroid of detected blobs in x and y coordinates (pixel) and the diameter of the blob (pixel). The obtained information is converted to an S.I. unit based on the image properties during the photographic process. The converted information has proceeded for the determination of raindrop size distribution. The raindrop size distribution of the images is co-related with the rainfall intensities recorded by the rain gauge. All the collected information is then compiled and calculated into the new rainfall factor (Equatorial Rainfall Erosivity Factor, R_{eqt}-factor).

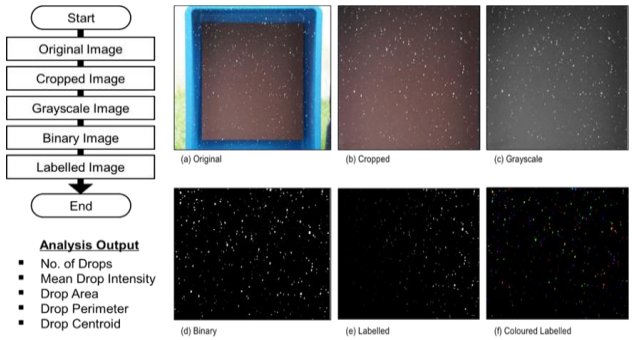

Fig. 4 Image processing for raindrop size distribution

3. Model Description and Formation

The research methodology focuses on developing a new soil loss equation called the Equatorial Soil Loss Equation (EQSLE). Some key determining factors have been considered during the research planning stage throughout the development process. Rainfall Erosivity Factor (R-factor) and Slope-Length Factor (LS-factor) are the main factors for the EQSLE. Both factors had dominated the soil erosion estimation with equatorial climate characteristics and the unique topographical conditions in the Borneo Highlands. The experiments' expected output includes rainfall intensity, soil loss rate, runoff coefficients, raindrop size distribution, particle size distribution, and other related analyses. The formation of EQSLE includes Equatorial Rainfall Erosivity Factor (R_{eqt}-factor), Equatorial Slope Length Factor (L_{eqt}-factor), Soil Erodibility Factor (K-factor), Crop Management Factor (C-factor) and Support Practices Factor (P-factor). The general framework for forming the equation is shown in Fig. 5.

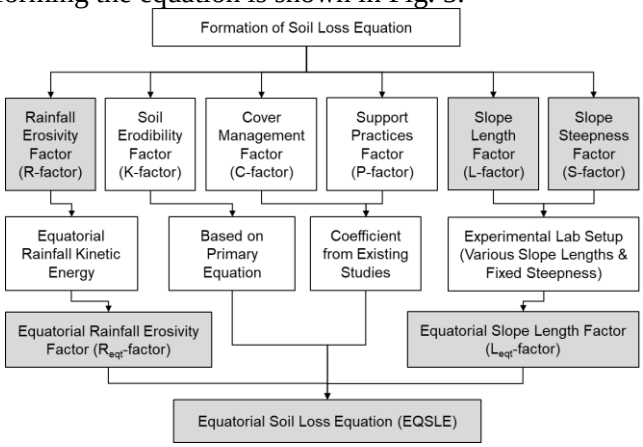

Fig. 5 Equation development framework

3.1. Equatorial Rainfall Erosivity Factor (R_{eqt}-Factor)

The relationship between rainfall kinetic energy and rainfall intensity is crucial and affects the prediction of soil loss. In this study, the analysis of rainfall kinetic energy begins with the properties of rainfall patterns during a storm event. The rainfall patterns include raindrop size distribution and raindrop sizes that lead to the estimations of the impact of raindrops on the surface ground. MATLAB was used to analyze the raindrop size properties and distribution patterns to

determine the relationship between rainfall kinetic energy and rainfall intensities. The rainfall photograph calibration was carried out to determine the raindrop capturing and analyzing process's performance. Optimization and conversion of raindrop size from the captured image to actual sizes must calculate raindrop sizes and distribution for specific rainfall intensities. Fig. 6 illustrates the flowchart for the formation of R_{eqt}-factor for rainfall intensities available throughout the experiments.

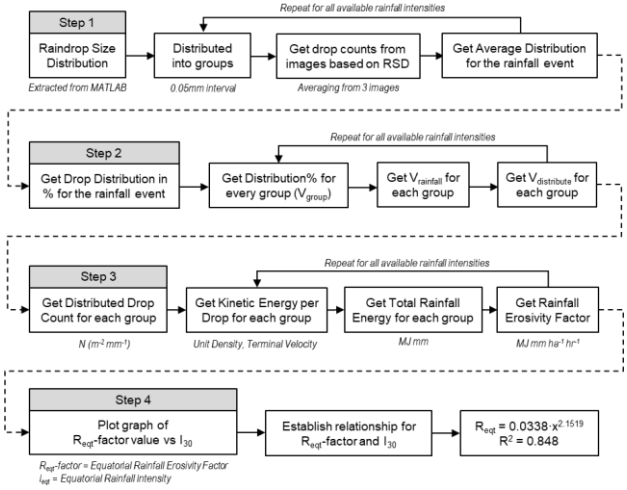

Fig. 6 Flowchart for the formation of R_{eqt}-factor

The redistribution of drop counts is an effective procedure to show the actual drop distribution within the storm event with reference to the captured distribution in MATLAB. The raindrop count was categorized according to the boundary conditions of the group assigned. The detected drop distribution is the expected drop distribution ratio based on the experimental condition, and it would require scaling up to the storm event quantity to estimate the rainfall kinetic energy of the storm event. The volume for the respective drop diameter groups can be determined by fractioning the distributed ratio by the total rainfall volume for the storm event. The determination of rainfall volume for the respective drop diameter groups can be accomplished using Equation (1), where V_{group} is the volume distributed to the drop diameter group (mm^3), $\%_{Distribution}$ is the drop distribution from the captured image (%), $V_{rainfall}$ is the total volume of the storm event (mm^3).

$$V_{group} = V_{rainfall} \times (\%_{Distribution}) \quad (1)$$

The shape of a raindrop is generally assumed as spherical. The volume of the raindrop group can then be divided by the volume per raindrop to obtain the number of drops for the raindrop group. The determination of the raindrop energy would be based on a similar fundamental as the kinetic energy equation. The kinetic energy can be determined using Equation (2).

$$KE_{drop} = \frac{1}{2} \cdot m_{drop} \cdot (v_{terminal})^2 \quad (2)$$

where KE_{drop} is the kinetic energy per raindrop (J), m_{drop} is the mass of the raindrop (kg), $v_{terminal}$ is the terminal velocity of a raindrop (m s^{-1}).

Based on the data obtained from the experimental trials, the relationship of total kinetic energy per rainfall depth (E) versus rainfall intensity (I_{30}) is demonstrated in the kinetic energy calculation section. For the equatorial rainfall erosivity factor (R_{eqt}-factor), the total kinetic energy per rainfall depth (E) can be replaced with E_{eqt} to represent total kinetic energy per rainfall depth, as measured in this study to mimic in equatorial rainfall intensities. R_{eqt}-factor is the combination of variable E_{eqt} (equatorial rainfall energy) and I_{eqt} (equatorial rainfall intensity), with the unit of megajoules per hectare per millimeter of rain (MJ ha^{-1} mm^{-1}) and millimeter per hour (mm hr^{-1}), respectively. The final unit for R_{eqt}-factor can be expressed as MJ mm ha^{-1} hr^{-1}. In this study, the energy content of the R_{eqt}-factor is plotted against rainfall intensities to R_{eqt}-factor derived as shown in Fig. 7.

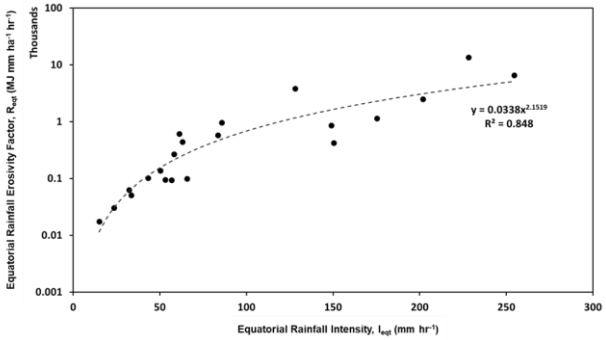

Fig. 7 Best fit of R_{eqt}-factor vs rainfall intensity

The relationship between R_{eqt} and E_{eqt}, and the simplified equation for R_{eqt} vs I_{eqt} can be written as shown in Equations (3) and Equation (4), where R_{eqt} is the equatorial rainfall erosivity factor (MJ mm ha^{-1} hr^{-1}), E_{eqt} is kinetic energy for rainfall in the equatorial region (MJ ha^{-1}), I_{eqt} is the equatorial rainfall intensity (mm hr^{-1}).

$$R_{eqt} = E_{eqt} \cdot I_{eqt} \quad (3)$$

$$R_{eqt} = 0.0338 \cdot {I_{30}}^{2.1519} \quad (4)$$

Based on the chart shown in Fig. 7, the Reqt-factor increases as the rainfall intensity increases; with 84.80% a positive linear relationship in the exponential best fits the graph. An increase in R-factor is expected because it is closely related to incremental in drop counts that would contribute to a significant increment in rain kinetic energy. The fundamentals of this new exponential equation can be constructed using an experimental test to simulation equatorial climate on the rainfall intensities up to 250 mm hr^{-1}.

3.2. Equatorial Slope Length Factor (L_{eqt}-Factor)

Topography is a significant factor affecting the outcome of soil erosion processes and it is essential to evaluate the effects of topography on erosion for soil erosion rate estimation. Slope Length Factor (L-factor) and Slope Steepness Factor (S-factor) affect the length.

The research timeline and funding constrain this experiment setup, so it is only available for one fixed angle (22.78°) in this experiment works. It is highlighted that it is specially focused on the hilly terrain commonly faced in Sarawak (>25° slope steepness) and provides constant factors on slope steepness to detail the changes and soil erosion outcomes [16, 17]. The modification of the L-factor focuses on the coefficient m, which dominates the outcomes without changing the fundamentals of the L-factor. Many researchers have conducted related studies and modifications regarding the coefficient, including [30] and the flowchart for forming L_{eqt}-factor illustrated in Fig. 8.

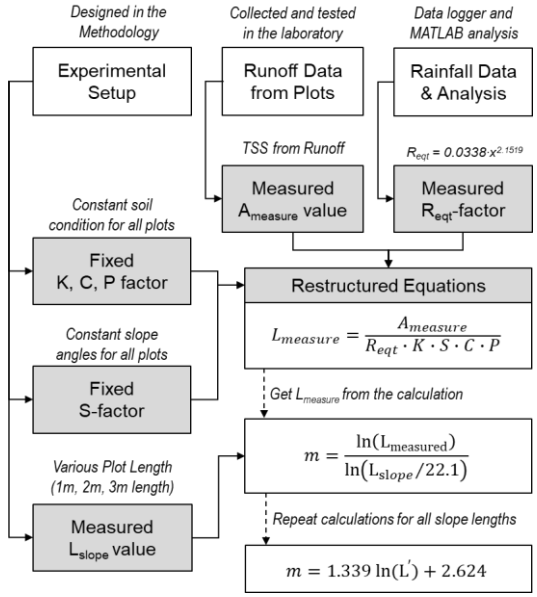

Fig. 8 Flowchart of or the formation of L_{eqt}-factor

The experimental setup was designed to ensure all the necessary factors are considered, including R, K, C, P, L, and S-factor. The runoff samples are collected after the rainfall event and Total Suspended Solids (TSS) is the important parameter that is taken and be converted to the erosion rate according to the plot sizes, rainfall intensities and rainfall volume collected. The TSS obtained from the data is derived to measure soil erosion rate ($A_{measure}$). Collected rainfall data with photogrammetric analysis are processed as measured equatorial rainfall erosivity factor (R_{eqt}-factor). Few soil conditions are fixed for all plots to ensure there is no external disturbance from other factors, including providing consistent soil type throughout the experiments (Soil Erodibility Factor, K-factor), ensuring bare soil condition on every plot (Cover Management Factor, C-factor) and no input of any soil erosion prevention method (Support Practices Factor, P-factor). Various plot lengths are designed for the studies of L-factor under the other fixed factors. Equatorial climate conditions are considered in the designed experiment, which is R_{eqt}-factor. The findings of the experiments would contribute to the development of Equatorial Slope Length Factor (L_{eqt}-factor). The previous S-factor equation developed by Wischmeier & Smith [31] is applied to a modified equation displayed in Equation (5) to obtain the measured L-factor based on the experimental data, where $L_{measured}$ is measured L-factor calculated from experimental data and $A_{measured}$ is measured soil erosion rate obtained from experimental data (t ha^{-1}).

$$L_{measured} = \frac{A_{measured}}{R_{eqt} \cdot K \cdot S \cdot C \cdot P} \quad (5)$$

A similar methodology was applied to data collected from three different plot lengths, including 1-m plot, 2-m plot and 3-m plot. The measured L-factor for three different plot lengths is applied to Equation (6) and a logarithmic relationship is plotted between the measured L-factor and slope length.

$$L_{measured} = \left(\frac{L_{length}}{22.1}\right)^{m} \quad (6)$$

Coefficient m is the key component that dominant the output of L-factor. The equation is re-structured to obtain various coefficients m based on the different conditions in Equation (7).

$$m = \frac{\ln(L_{measured})}{\ln(L_{slope}/22.1)} \quad (7)$$

Many different outcomes have been recorded and considered throughout the experiments. The $L_{measured}$ for all plots are recorded and the outputs for coefficient *m* are plotted into a graph with respect to the rainfall intensities, according to three different plot lengths. This step is to determine the co-relationship of the coefficient *m* and the various plot lengths. The relationship is established into Equation (8), where L_{eqt} is the Equatorial Slope Length Factor, L_{slope} is slope length (m), m_{eqt} is the coefficient for L_{eqt}-factor.

$$L_{eqt} = \left(\frac{L_{slope}}{22.1}\right)^{m_{eqt}}, \quad (8)$$

where $m_{eqt} = 1.339\, ln(L_{slope}) + 2.624$

3.3. Soil Erodibility Factor (K-Factor)

Soil erodibility factor (K-factor) is the only factor subjected to the condition of the surface soil that experiences erosion. [6] derived the K-factor, a soil erodibility model that relies on the soil composition related to the soil particles' detachment during erosion. With the changes in surface soil types, the K-factor can still be determined based on the composition and the soil properties. The equation to determine the K-factor is shown in Equation (9) and Equation (10), where K is the soil erodibility factor (t ha hr ha^{-1} MJ^{-1} mm^{-1}), f_p is the particle size parameter, P_{om} is the percent organic matter, S_{struc} is the soil structure index, f_{perm} is the profile-permeability class factor, P_{clay} is the percent clay, P_{silt} is the percent silt.

$$K = 2.1 \times 10^{-6} \cdot f_p^{\,1.14}(12 - P_{om}) + 0.0325(S_{struc} - 2) + 0.025(f_{perm} - 3) \quad (9)$$

$$f_p = P_{silt}(100 - P_{clay}) \quad (10)$$

3.4. Cover Management Factor (C-Factor) and Support Practices Factor (P-Factor)

The experimental setup for the plot is designed as bare soil for the plots. The setting of the soil surface for the plot is designed to be filled soil (loosen soil) with a fairly compacted surface, which is smooth and flat on the surface soil. The C-factor is the effectiveness of cropping on changes in erosion rates, while the P-factor is the ratio of soil loss with a specific soil erosion reduction method at a specific site under study [7]. [32] justified that the C-factor needs to be further researched because lacking incorporation or inclusion of some elements for the C-value. For instance, a long-term monitoring period must determine representative C-values. The P-factor is based on the USLE, but the data are limited. Similarly, the determination of P-values would require an extended monitoring period.

3.5. Equatorial Soil Loss Equation (EQSLE)

The most significant factor in this study, R-factor and L-factor is developed experimentally based on the climate in the equatorial region, and a new form of R-factor and L-factor are derived, called Equatorial Rainfall Erosivity Factor (R_{eqt}-factor) in Equation (4) and Equatorial Slope Length Factor (L_{eqt}-factor) in Equation (8). With the combination of the other soil loss factors, the newly formed soil loss equation is named Equatorial Soil Loss Equation (EQSLE), as shown in Equation (11).

$$A_{eqt} = R_{eqt} \cdot L_{eqt} \cdot S \cdot K \cdot C \cdot P \quad (11)$$

$$R_{eqt} = 0.0338 \cdot {I_{30}}^{2.1519} \quad (4)$$

$$L_{eqt} = \left(\frac{L_{slope}}{22.1}\right)^{m_{eqt}},$$

$$\text{where } m_{eqt} = 1.339\, ln\left(L_{slope}\right) + 2.624 \quad (8)$$

A_{eqt} is equatorial soil loss rate (t ha^{-1}), R_{eqt} is equatorial rainfall erosivity factor (MJ mm ha^{-1} hr^{-1})h L_{eqt} is the equatorial slope length factor, S is the equatorial slope steepness factor, C is the cover management factor and P is the support practice factor. The value can be determined based on the requirements and conditions of the respective factors. The sequences of assessing the value of the soil loss factors are demonstrated in the previous section, and similar methods can be applied to any site for soil loss rate estimation. The main goal of this study up to the current progress is to derive EQSLE. The main highlight for EQSLE is the potential of the soil loss equation that it could perform soil loss rate estimation with higher accuracy and more reasonable prediction for any site located in the equatorial region.

4. Results and Discussion

4.1. Comparison of R-Factor

A comparison of R values against measured R values was carried out between EQSLE R-factor, R equation [6] and the R equation [7]. The graph for three different R-value comparisons is plotted in Fig. 9. The difference between [6] and [7] is significant as they are the pioneers that contributing to soil erosion studies with respect to rainfall intensities. The plotted points of R values by EQSLE are more concentrated around the reference line with reference to the measured R values. This suggests that the R values by EQSLE displayed close estimation compared to experimental data. This finding highlights that the R_{eqt}-factor by EQSLE is applicable and practical to be practiced for any soil erosion assessment. R equation in [6] and R equation in [7] provided similar output against the measured R values. The readings for R values in [6] and in [7] show a substantially different compared to the experimental data. A scatter plot away from the reference line suggested that the outcomes were less reliable for the R-factor value calculations for soil erosion assessment events.

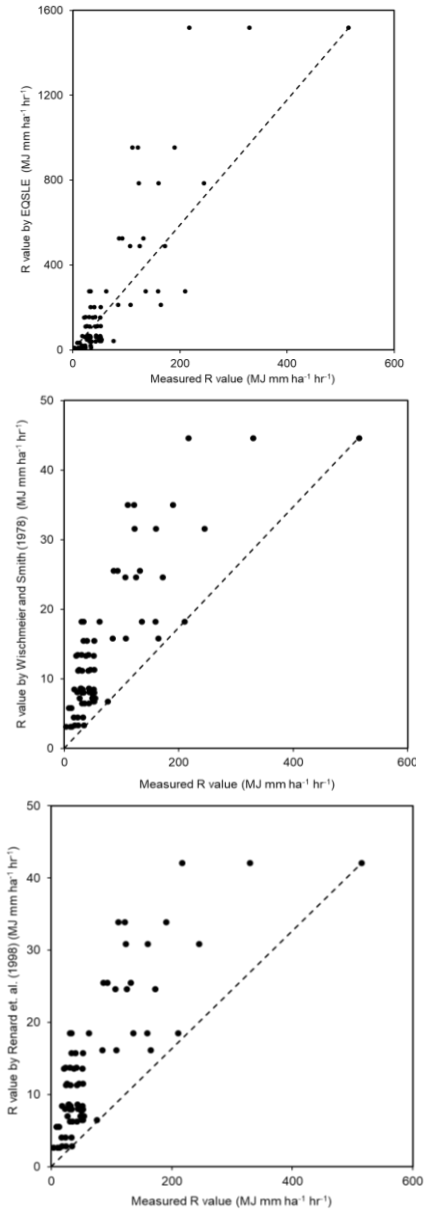

Fig. 9 R-value by EQSLE, [6] and [7] versus measured R-value

4.2. Comparison of LS-Factor

Two different LS values were compared for this study: the LS-value by EQSLE and the LS-value

developed in [33]. It is preferable to look at the L and S-factor into a single chart to better present the factors. The LS chart by EQSLE and [33] is illustrated in Fig. 10 and Fig. 11. The two LS charts have different graph behavior. The different graph behavior might be due to the formation of the equation format initiated by the empirical studies of the soil erosion data. Researchers have different formats to present their LS chart, but LS-value in [33] is typically the chart type practiced by the current research and industrial practitioners. A high increment of the gradient in the section from 0 m to 3-m slope length exists. A slow increment of LS-value with the increment of slope length and this scenario happens for all slope steepness. This is understandable for the sharp increment of the data because, based on the empirical databases; such a short slope might be challenging to have sufficient data to provide a good output on the graph.

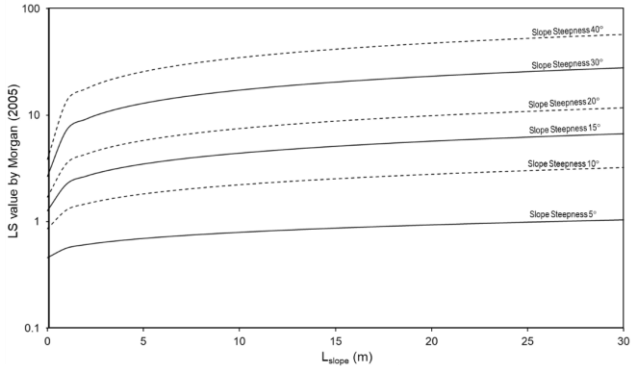

Fig. 10 LS values by [33]

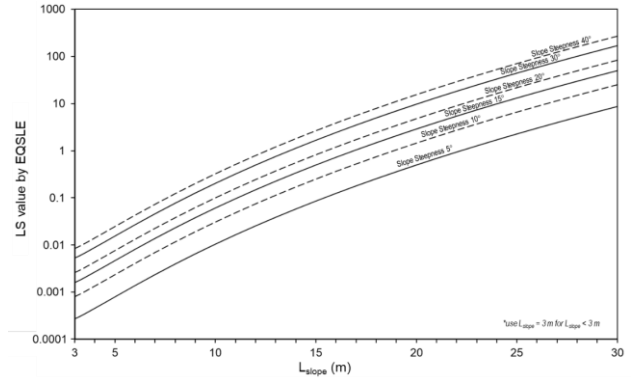

Fig. 11 LS value chart for EQSLE

A more detailed study of shorter slope length was conducted for L_{eqt}-factor and it is present in the LS chart by EQSLE (Fig. 11). It is highlighted that the value for shorter slope length is provided with more detail than that in [33]. The authors had proposed a limitation to the LS-factor by EQSLE. Slope lengths shorter than 3 m could not be displayed on the graph due to the logarithm graph behavior. Considering the values tabulated by slope length more than 3 m, it is recommended to adopt the value of LS-factor where the L_{slope} is 3 m. The LS-value for slope length more than 3 m and the LS-value for slope length of 3 m have minor differences. It is more conservative to adopt a value for the slope length of 3 m and it has been simplified to a more precise value compared to [33].

The LS-value by EQSLE and [33] shows a difference in value for a longer slope length and a shorter slope length. The LS-value by EQSLE is produced by developing local slope length data in both experimental and numerical methods. The LS-value [33] underestimates the suitable LS-value for the longer slope lengths and a minor overestimation for shorter slope lengths compared to LS-value by EQSLE. Note that this is a comparison between LS-value for both factors only. The overall estimation of soil erosion still must consider the other factors, including Rainfall Erosivity Factor (R-factor), Soil Erodibility Factor (K-factor), Cover Management Factor (C-factor) and Support Practices Factor (P-factor). The current differences in one factor might be due to the differences during the formation and development methods of the equation. This condition would only allow comparison the values in terms of magnitude and differences, but it is not meant to propose a universal solution for all soil erosion problems.

5. Conclusion

The main finding of this study focused on the comparison results for the current soil loss equation (EQSLE), R-factor and L-factor with other soil loss equation. The EQSLE was compared with the Revised Universal Soil Loss Equation (RUSLE) regarding the R and L factors. Experimentally, the EQSLE R_{eqt}-factor should be the more acceptable for equatorial climate, with a relatively simplified version of derivation and would resolve rainfall intensity limitations compared to RUSLE R-factor. This answered the objectives of this research to experimentally derive R-factor for equatorial climate and the equatorial soil loss equation for the development sites in the equatorial region. The EQSLE L_{eqt}-factor has primarily resolved the soil erosion issue in Sarawak for hilly and mountainous terrains with high equatorial annual precipitation. The application of EQSLE would help improve the accuracy of the soil loss estimation and thus reduce additional costing and time required to provide an optimized solution for Erosion and Sediment Control Plan (ESCP). The challenge in this study is the limited improvement of soil loss estimation precision under the changes in climate condition, such as the increases in rainfall intensities, where the EQSLE could only be able to handle up to 250 mm hr^{-1} of maximum rainfall intensity. For future recommendation, the EQSLE shall be applied in more case studies on its performance on soil loss rate prediction. More studies on different slope angles are recommended in future work to improve the overall LS-factor performance for soil erosion estimation in the equatorial region. The other soil loss factors would be required to have more profound research when more research data are available to justify the derivations.

Acknowledgment

The authors want to thank the Fundamental Research Grant Scheme (FRGS) (Reference Code: FRGS/1/2019/TK01/SWIN/02/1) by the Ministry of Education Malaysia for supporting this research project.

References

[1] SMITH H.J. Application of Empirical Soil Loss Models in southern Africa: A review. *South African Journal of Plant and Soil*, 1999, 16(3): 158-163. 10.1080/02571862.1999.10635003.

[2] NEARING M., FOSTER G., LANE L., and FINKNER S. A process-based soil erosion model for USDA-water erosion prediction project technology, *Soil and Water Division of ASAEL*, 1989, 32(5): 1587-1593.

[3] MISRAA R.K., and ROSE C.W. Application and sensitivity analysis of process-based erosion model GUEST. *European Journal of Soil Science*., 1996, 47: 593-604.

[4] MORGAN R.P.C., QUINTON J.N., SMITH R.E., GOVERS G., A. POESEN J.W., AUERSWALD K., CHISCI G., TORRI D., and STYCZEN M.E. The European Soil Erosion Model (EUROSEM): A Dynamic Approach For Predicting Sediment Transport From Field And Small Catchments. *Earth Surface Processes and Landforms*, 1998, 544(23): 527-544.

[5] DE ROO A.P.J. The LISEM Project: An Introduction, *Hydrological Processes*, 1996, 10: 1021-1025.

[6] WISCHMEIER W.H., and SMITH D.D. P*redicting Rainfall Erosion Losses – A Guide to Conservation Planning*, U.S. Department of Agriculture, 1978.

[7] RENARD K.G., FOSTER G.R., WEESIES G.A., MCCOOL D.K., and YODER D.C. *Predicting soil erosion by water: A guide to conservation planning with the revised universal soil loss equation (RUSLE)*. U.S. Government Printing Office, 1998.

[8] RISSE L.M., NEARING M.A., LAFLEN J.M., and NICKS A.D. Error Assessment in the Universal Soil Loss Equation. *Soil Science Society of America Journal*, 1993, 57(3): 825-833.

[9] ONSTEAD C.A., PIEST R.F., and SAXTON K.E. Watershed Erosion Model Validation for Southwest Iowa. In: *The Third Federal Inter-Agency Sedimentation Conference*, 1976: 1-22.

[10] ALBALADEJO MONTORO J. and STOCKING M. Comparative evaluation of two models in predicting storm soil loss from erosion plots in semi-arid Spain, *Catena*, 1989, 16 (3): 227-236.

[11] KRAMER L.A., and ALBERTS E.E. C Factors for Corn Under Changing Management. *Transactions of the American Society of Agricultural Engineers*, 1986, 29(6): 1590-1596.

[12] FREEBAIRN D.M., SILBURN D.M., and LOCH R.J. Evaluation of Three Soil Erosion Models for clay Soils. *Australian Journal of Soil Research*, 1989, 27: 199-211.

[13] WELTZ M.A., RENARD K.G., and SIMANTON J.R. Revised Universal Soil Loss Equation for Western Rangelands. In: *USA/Mexico Symposium of Strategies for Classification and Management of Native Vegetation for Food Production in Arid Zones*. Tucson, USA., 1987.

[14] OSBORN H.B., SIMANTON J.R., and RENARD K.G. Use of the universal soil loss equation in the semiarid Southwest. Soil Erosion: Prediction and Control. *Journal of Soil and Water Conservation*, 1976, 21: 41-49.

[15] TRIESTE D.J., and GIFFORD G.F. Application of the Universal Soil Loss Equation to Rangelands on a Per-Storm Basis. *Journal of Range Management*, 1980, 33(1): 66.

[16] YAMAKURA T., KANZAKI M., ITOH A., OHKUBO T., OGINO K., CHAI E.O.K., LEE H.S., and ASHTON P.S. Topography of a Large-Scde Research Plot Established within a Tropical Rain Forest at Lambir, Sarawak. *Tropics*, 1995, 5(2): 41-56.

[17] ITOH A., YAMAKURA T., OHKUBO T., KANZAKI M., POLIMIOTTO P.A., LAFRANKIE J.V., ASHTON P.S., and LEE H.S. Importance of topography and soil texture in the spatial distribution of two sympatric dipterocarp trees in a Bornean rainforest. *Ecological Research*, 2003, 18(3): 307-320.

[18] GOH E., and TEW K.H. *Soil erosion engineering : reliability-based engineering design, soil erosion assessment and best practices*. Publisher of Universiti Sains Malaysia, Penang, Malaysia, 2006.

[19] SUJAUL I.M., BARZANI G.M., ISMAIL B.S., SAHIBIN A.R., and EKHWAN T.M. Estimation of the rate of soil erosion in the Tasik Chini Catchment, Malaysia using the RUSLE model integrated with the GIS. *Australian Journal of Basic and Applied Sciences*, 2012, 6(12): 286-296.

[20] GREGERSEN B., LAURIDSEN P.E., KAAS M., LOPDRUP U., and VAN DER KEUR P. Land Use and Soil Erosion in Tikolod, Sabah, Malaysia. *ASEAN Review of Biodiversity and Environmental Conservation*, 2003, March: 1-11.

[21] ABIDIN R.Z., and TEW K.H. *Evaluation of soil erosion features along the North - South expressway (Bukit Kayu Hitam - Johor Bahru)*. VT Soil Erosion Research & Consultancy, Malasia, 2000.

[22] LAW S.L.G., and KUOK K.K. Sensitivity Analysis of the Revised Universal Soil Loss Equation's Rainfall Erosivity Factor (R-Factor). *Test Engineering and Management*, 2020, 83(May-June): 6809-6815.

[23] KUEH S.M., and KUOK K.K. Precipitation Downscaling Using The Artificial Neural Network Batnn and Development of Future Rainfall Intensity-Duration-Frequency Curves. *Climate Research*, 2016, 68(1): 73-89.

[24] WONG C.L., VENNEKER R., UHLENBROOK S., JAMIL A.B.M., and ZHOU Y. Variability of rainfall in Peninsular Malaysia. *Hydrology and Earth System Sciences Discussions*, 2009, 6: 5471-5503.

[25] CHIU P.C., SELAMAT A., KREJCAR O., and KUOK K.K. Missing rainfall data estimation using artificial neutral network and nearest neighbour imputation. In: *SoMeT*, Sarawak, Malaysia, 2019: 132-143.

[26] TENG Y.H., KUOK K.K., IMTEAZ M., LAI W.Y., and XIONG K. Development of Whale Optimization Neural Network for Daily Water Level Forecasting. In: *The 10th International Conference on Computing, Technology and Engineering, Kuala Lumpur, Malaysia*, 2019.

[27] KOTTEK M., GRIESER J., BECK C., RUDOLF B., and RUBEL F. World Map of The Köppen-Geiger Climate Classification Updated. *Meteorological Journal*, 2006, 15(3): 259-263.

[28] KUOK K.K., MAH Y.S., IMTEAZ M.A., and KUEH S.M. Comparison of Future Intensity Duration Frequency Curve By Considering The Impact of Climate Change: Case Study for Kuching City. *Journal of River Basin Management*, 2016, 14(1): 47-55.

[29] LAW S.L.G., KUOK K.K., and GATO-TRINIDAD S. An Experimental Study on The Correlation of Natural Rainfall Intensities and Raindrop Size Distribution Characteristics. *IOP Conference Series: Materials Science and Engineering*, 2021, 1101(1): 012009.
[30] QIN W., GUO Q.K., CAO W.H., YIN Z., YAN Q.H., SHAN Z.J., and ZHENG F.L. A New RUSLE slope length factor and its application to soil erosion assessment in a Loess Plateau watershed. *Soil and Tillage Research*, 2018, 182: 10-24. DOI: 10.1016/j.still.2018.04.004
[31] WISCHMEIER W.H., and SMITH D.D. *Predicting Rainfall Erosion Losses A Guide to Conservation Planning*. Science and Education Administration, U.S. Department of Agriculture, 1987.
[32] HUDSON N. *Field Measurement of Soil Erosion and Runoff*. Food and Agriculture Organization of the United Nations, Rome, 1993.
[33] MORGAN R.P.C. *Soil Erosion and Conservation*, 3rd ed. Baclkwell Publishing Ltd, MA, USA, 2005.
[34] MAXWELL J.B. Climatic Regions of the Canadian Arctic Islands. *Arctic*, 1981, 34(3): 225-240.
[35] OHMURA A., and REEH N. New precipitation and accumulation maps for Greenland. *Journal of Glaciology*, 1991, 37: 140-148.
[36] VAN DIJK, BRUIJNZEEL, and ROSEWELL. Rainfall intensity–kinetic energy relationships: a critical literature appraisal. *Journal of Hydrology*, 2002, 261: 1-23.
[37] ANDRONACHE C. Estimates of sulfate aerosol wet scavenging coefficient for locations in the Eastern United States. *Atmospheric Environment*, 2004, 38(6): 795-804.
[38] ALVARES C.A., STAPE J.L., SENTELHAS P.C., DE MORAES GONCALVES J.L., and SPAROVEK G. Köppen's climate classification map for Brazil. *Meteorological Journal*, 22(6): 711-728.
[39] PEEL M.C., FINLAYSON B.L., and MCMAHON T.A. Updated world map of the Köppen-Geiger climate classification. *Hydrology and Earth System Sciences*, 2007, 11: 1633–1644.
[40] LAL R. A soil suitability guide for different tillage systems in the tropics. *Soil and Tillage Research*, 1985, 5(2): 179-196.
[41] JACKSON I.J. *Climate, water and agriculture in the tropics*. Longman, London, New York, N.Y., 1977.

参考文:

[1] SMITH H.J. 經驗土壤流失模型在南部非洲的應用：綜述。 南非植物與土壤雜誌，1999年，16(3)：158-163。10.1080/02571862.1999.10635003。
[2] NEARING M., FOSTER G., LANE L. 和 FINKNER S. 美國農業部水土流失預測項目技術的基於過程的土壤侵蝕模型，*ASAEL*水土司, 1989, 32(5): 1587-1593。
[3] MISRAA R.K. 和 ROSE C.W. 基於過程的侵蝕模型格里菲斯大學侵蝕系統模板的應用和敏感性分析。歐洲土壤科學雜誌，1996年，47：593-604。
[4] MORGAN R.P.C.、QUINTON J.N.、SMITH R.E.、GOVERS G.、A. POESEN J.W.、AUERSWALD K.、CHISCI G.、TORRI D. 和 STYCZEN M.E. 歐洲土壤侵蝕模型：動態預測方法來自田間和小集水區的泥沙輸送。地表過程與地貌, 1998, 544(23): 527-544.
[5] DE ROO A.P.J. LISEM 項目：簡介，水文過程，1996年，10：1021-1025。
[6] WISCHMEIER W.H. 和 SMITH D.D.預測降雨侵蝕損失——保護規劃指南，美國農業部，1978年。
[7] RENARD K.G.、FOSTER G.R.、WEESIES G.A.、MCCOOL D.K. 和 YODER D.C. 預測水土流失：使用修訂後的通用土壤流失方程進行保護規劃的指南。美國政府印刷局，1998年。
[8] RISSE L.M.、NEARING M.A.、LAFLEN J.M. 和 NICKS A.D. 通用土壤流失方程中的誤差評估。美國土壤學會雜誌，1993年，57(3)：825-833。
[9] ONSTEAD C.A.、PIEST R.F. 和 SAXTON K.E.愛荷華州西南部流域侵蝕模型驗證。在：第三屆聯邦機構間沉積會議，1976年：1-22。
[10] ALBALADEJO MONTORO J. 和 STOCKING M. 西班牙半乾旱地區侵蝕地塊風暴土壤流失預測的兩種模型比較評價, 系列, 1989, 16 (3): 227-236.
[11] KRAMER L.A. 和 ALBERTS E.E. 改變管理下玉米的 C 因素。美國農業工程師學會彙刊，1986年，29(6)：1590-1596。
[12] FREEBAIRN D.M.、SILBURN D.M. 和 LOCH R.J.粘土三種土壤侵蝕模型的評價。澳大利亞土壤研究雜誌，1989年，27：199-211。
[13] WELTZ M.A.、RENARD K.G. 和 SIMANTON J.R. 修訂了西部牧場的通用土壤流失方程。在：美國/墨西哥乾旱地區糧食生產原生植被分類和管理戰略研討會。圖森，美國，1987年。
[14] OSBORN H.B.、SIMANTON J.R. 和 RENARD K.G. 通用土壤流失方程在西南半乾旱地區的應用。土壤侵蝕：預測和控制。水土保持學報, 1976, 21: 41-49.
[15] TRIESTE D.J. 和 GIFFORD G.F.在每次風暴的基礎上將通用土壤流失方程應用於牧場。牧場管理雜誌, 1980, 33(1): 66.
[16] YAMAKURA T.、KANZAKI M.、ITOH A.、OHKUBO T.、OGINO K.、CHAI E.O.K.、LEE H.S. 和 ASHTON P.S. 在砂拉越蘭比爾的熱帶雨林內建立的大型研究地塊的地形。熱帶, 1995, 5(2): 41-56.
[17] ITOH A.、YAMAKURA T.、OHKUBO T.、KANZAKI M.、POLIMIOTTO P.A.、LAFRANKIE J.V.、ASHTON P.S. 和 LEE H.S. 地形和土壤質地在婆羅洲雨林中兩種同域龍腦香樹空間分佈中的重要性。生態研究, 2003, 18(3): 307-320.
[18] GOH E. 和 TEW K.H. 土壤侵蝕工程：基於可靠性的工程設計、土壤侵蝕評估和最佳實踐。馬來西亞理科大學出版社，馬來西亞檳城，2006年。
[19] SUJAUL I.M.、BARZANI G.M.、ISMAIL B.S.、SAHIBIN A.R. 和 EKHWAN T.M.使用與地理信息系统集成的魯斯勒模型估算馬來西亞奇尼湖集水區的土壤侵蝕率。澳大利亞基礎與應用科學雜誌，2012年，6(12)：286-296。
[20] GREGERSEN B.、LAURIDSEN P.E.、KAAS M.、LOPDRUP U. 和 VAN DER KEUR P. 馬來西亞沙巴提科洛德的土地利用和土壤侵蝕。東盟生物多樣性和環境保護評論，2003年3月：1-11。
[21] ABIDIN R.Z. 和 TEW K.H. 評估南北高速公路（武吉加由黑淡 - 新山）沿線的土壤侵蝕特徵。VT土壤侵蝕研究與諮詢公司，馬來西亞，2000年。
[22] LAW S.L.G. 和 KUOK K.K. 修訂後的通用土壤流失方程的降雨侵蝕係數（R係數）的敏感性分析。測試工

程與管理, 2020, 83(5-6月): 6809-6815.
[23] KUEH S.M. 和 KUOK K.K. 使用人工神經網絡模式的降水降尺度和未來降雨強度-持續時間-頻率曲線的開發。氣候研究, 2016, 68(1): 73-89.
[24] WONG C.L.、VENNEKER R.、UHLENBROOK S.、JAMIL A.B.M. 和 ZHOU Y. 馬來西亞半島降雨量的變化。水文學與地球系統科學討論, 2009, 6: 5471-5503.
[25] CHIU P.C.、SELAMAT A.、KREJCAR O. 和 KUOK K.K. 使用人工中性網絡和最近鄰插補的缺失降雨數據估計。在：SoMeT，馬來西亞砂拉越，2019年：132-143。
[26] TENG Y.H., KUOK K.K., IMTEAZ M., LAI W.Y. 和 XIONG K. 用於每日水位預報的鯨魚優化神經網絡的開發。在：第十屆計算、技術與工程國際會議，馬來西亞吉隆坡，2019年。
[27] KOTTEK M.、GRIESER J.、BECK C.、RUDOLF B. 和 RUBEL F. 柯本蓋格氣候分類世界地圖已更新。氣象雜誌, 2006, 15(3): 259-263.
[28] KUOK K.K.、MAH Y.S.、IMTEAZ M.A. 和 KUEH S.M. 考慮氣候變化影響的未來強度持續時間頻率曲線比較：古晉市案例研究。流域管理學報, 2016, 14(1): 47-55.
[29] LAW S.L.G.、KUOK K.K. 和 GATO-TRINIDAD S. 自然降雨強度與雨滴大小分佈特徵相關性的實驗研究。物理研究所會議系列：材料科學與工程, 2021, 1101(1): 012009.
[30] QIN W., GUO Q.K., CAO W.H., YIN Z., YAN Q.H., SHAN Z.J., 和 ZHENG F.L.一種新的魯斯勒坡長因子及其在黃土高原流域土壤侵蝕評價中的應用.土壤與耕作研究, 2018, 182: 10-24. DOI：10.1016/j.still.2018.04.004
[31] WISCHMEIER W.H. 和 SMITH D.D.預測降雨侵蝕損失保護規劃指南。美國農業部科學與教育管理局，1987年。
[32] HUDSON N. 土壤侵蝕和徑流的現場測量。聯合國糧食及農業組織，羅馬，1993年。
[33] MORGAN R.P.C. 土壤侵蝕與保護，第3版。貝克韋爾出版有限公司，美國馬薩諸塞州，2005年。
[34] MAXWELL J.B. 加拿大北極群島氣候區。北極, 1981, 34(3): 225-240。
[35] OHMURA A. 和 REEH N. 格陵蘭的新降水和累積圖。冰川學報, 1991, 37: 140-148.
[36] VAN DIJK, BRUIJNZEEL 和 ROSEWELL。降雨強度-動能關係：一項批判性文獻評價。水文雜誌, 2002, 261: 1-23.
[37] ANDRONACHE C. 美國東部地區硫酸鹽氣溶膠濕清除係數的估計。大氣環境, 2004, 38(6): 795-804.
[38] ALVARES C.A.、STAPE J.L.、SENTELHAS P.C.、DE MORAES GONCALVES J.L. 和 SPAROVEK G. 科彭的的巴西氣候分類地圖。氣象雜誌，22(6)：711-728。
[39] PEEL M.C.、FINLAYSON B.L. 和 MCMAHON T.A. 更新了柯本蓋革氣候分類的世界地圖。水文學與地球系統科學, 2007, 11: 1633–1644.
[40] LAL R. 熱帶地區不同耕作系統的土壤適宜性指南。土壤與耕作研究, 1985, 5(2): 179-196.
[41] JACKSON I.J. 熱帶地區的氣候、水和農業。朗文出版社，倫敦，紐約，紐約州，1977年。